CONTINUOUS CLOUD LIDAR MONITORING AT SOUTH POLE STATION: ANALYSIS OF PSC FORMATION AND DENITRIFICATION POTENTIAL DURING 2003

James R. Campbell* and Kenneth Sassen
Dept. of Atmospheric Sciences, Univ. of Alaska-Fairbanks, Fairbanks, Alaska, USA

Ellsworth J. Welton and James D. Spinhirne
NASA Goddard Space Flight Center, Greenbelt, MD, USA

1. INTRODUCTION

Polar stratospheric clouds (PSC) are an artifact of extremely cold temperatures that occur in the lower stratosphere in the absence of sunlight during winter. Their presence induces chemical imbalances that influence catalytic ozone destruction initiated by the return of sunlight in spring long after the clouds disappear. Denitrification through cloud sedimentation leads to increased concentrations of chlorine and bromine radicals that fuel these reactions. Annual ozone "holes" (columns of ozone-poor concentration) develop in both hemispheres that are advected as far as the midlatitudes. Increased transmission of ultraviolet radiation resulting from ozone loss modifies surface radiation balance and may negatively affect the health of terrestrial organisms.

In this paper we discuss PSC observations made from the Scott/Amundsen South Pole station during austral winter 2003 with a micropulse lidar (MPL; 0.523 μm). PSC occurrence is more common in the southern hemisphere than in the Arctic. Persistence of the polar-night vortex over Antarctica generates sufficiently cold lower-stratospheric temperatures between May and September. Episodic lidar measurements of Antarctic PSC have previously been made from McMurdo, Rothera, Syowa and South Pole stations. The MPL data are unique. The instrument is eye-safe [*Campbell et al.*, 2001] and has operated continuously and autonomously from December 1999 to the present.

2. DATA PROCESSING

MPL data from South Pole are recorded at 60 s and 30 m resolution settings. Algorithms outlined by *Campbell et al.* [2001] and *Welton and Campbell* [2001] are used to process the raw signal to uncalibrated backscatter, including signal uncertainties. To increase signal-to-noise performance and improve retrievals from the lower-stratosphere the data are grouped into approx. 15-minute averages (0.01 fractional days). Using techniques outlined by *Campbell et al.* [2002] the data are normalized to a molecular scattering profile (derived from a polar-winter standard atmosphere) when possible using segments of particulate-free scatter nearest to the surface as possible.

Cloud boundaries are determined by examining signal strength relative to the uncertainty of the normalized profile calculated under the assumption of clear sky. The attenuated backscatter ratio (ABR) is defined as

$$ABR(z) = \frac{\left(\beta_m(z) + \beta_p(z)\right)T_m(z)^2 T_p^*(z^*)^2}{\beta_m(z)T_m(z)^2} \geq 1 \quad \textbf{(1)}$$

Here, β_m and β_p are the molecular and particulate backscatter coefficients, T_m^2 and T_p^2 are the corresponding column-transmission terms, and all are a function of height, z. Attenuated ratios refer to the influence of the particulate transmission term, from above the region chosen as "clear-sky" used to normalize the profile (denoted by T_p^*). As a function of signal uncertainties the cloud algorithm is limited to a minimum detectable ABR increasing non-linearly from 1.1 to near 4.0 between 10 and 25 km MSL.

3. DISCUSSION

In Fig. 1 ABR values for May – October 2003 are shown between 10 and 25 km MSL. The data have been smoothed to 1 day and 0.25 km resolution, using a two-dimensional Hanning window, with a 5 day and 0.75 km filter [*e.g., Pfenninger et al.*, 1999]. It is not immediately clear which clouds in Fig. 1 are PSC and which are generated by upper-tropospheric disturbances. The four ABR maxima (values between 2.0 and

* *Corresponding author address:* James R. Campbell, c/o Dept. of Atmospheric Sciences, Univ. of Alaska-Fairbanks, PO Box 757320, Fairbanks, AK 20771; *e-mail*: campbell@gi.alaska.edu

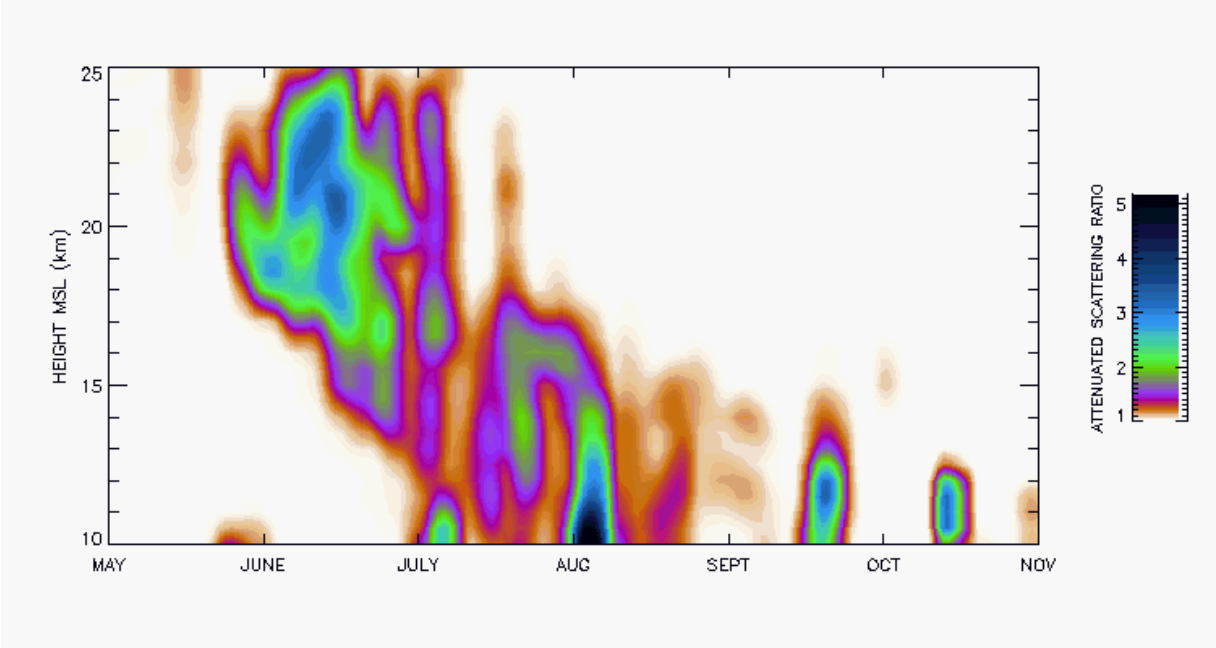

Figure 1. Attenuated backscatter ratios derived from micropulse lidar observations at South Pole from 10 to 25 km MSL between May and October 2003. The data have been smoothed to 1 day and 0.25 km resolution using a two-dimensional Hanning window with a 5 day and 0.75 km filter.

5.0) centered above 10 km between July and October reflect upper-tropospheric events as diagnosed with synoptic charts. Their influence is not seen above 15 km, however, and this level serves an approximate threshold here for distinguishing PSC.

In Fig. 2 are condensation and frost-point depressions for hypothetical nitric-acid trihydrate (12.0, 10.0, 8.0 ppbv with 4.0 ppmv water vapor; right) and water vapor mixing ratios (6.0, 4.0 and 2.0 ppmv; left). We use these compounds to represent Type I and Type II PSC respectively [*Toon et al.*, 1989]. Radiosonde launches occur daily from South Pole, however many balloons fail to reach the stratosphere during the cold winter months. Only those reaching 15 km MSL were included in this sample. Since this limited the dataset a Hanning window was applied to smooth the data to 1 day and 0.05 km resolution using a 14 day and 2 km temporal and spatial filter. There is only a 1 K condensation point difference for nitric-acid trihydrate between 8.0 and 12.0 ppbv. The difference in frost-point temperature for water vapor between 2.0 and 6.0 ppmv is approximately 7 K.

MPL observations suggest that dehumidification and denitrification occurred over South Pole in 2003. From Fig. 1 PSC were first observed between 17 and 25 km MSL, beginning in late May. The clouds persisted through early July. ABR maxima occurred during this period above 20 km MSL. These observations correlate well with the calculations in Fig. 2 for high water vapor and each of the nitric-acid concentrations. It is likely that these maxima represent Type II PSC. Ice was likely present throughout other regions of the cloud given ABR values uniformly above 2.0. After this period PSC were not observed above 17 km through August and 15 km for the remainder of the season despite the coldest temperatures being observed in early August near 20 km. ABR maxima near 2.0 were measured at 16 km in late July. Another peak occurred near 14 km around the same time. Frost-point depressions for 2 ppmv suggest ice-phase PSC possible up to 20 km through the middle of August. Similar calculations for nitric-acid suggest Type I PSC possible through most of the column into September. No such clouds were detected.

The strength of the polar vortex is a primary influence on the magnitude of dehumidification and denitrification of the lower stratosphere. Sedimentation of PSC will naturally lessen water vapor and nitrogen-based compound concentrations at specific heights. As flow around the vortex approaches geostrophic balance meridional mixing weakens. Vertical mixing is limited because of large-scale subsidence in the

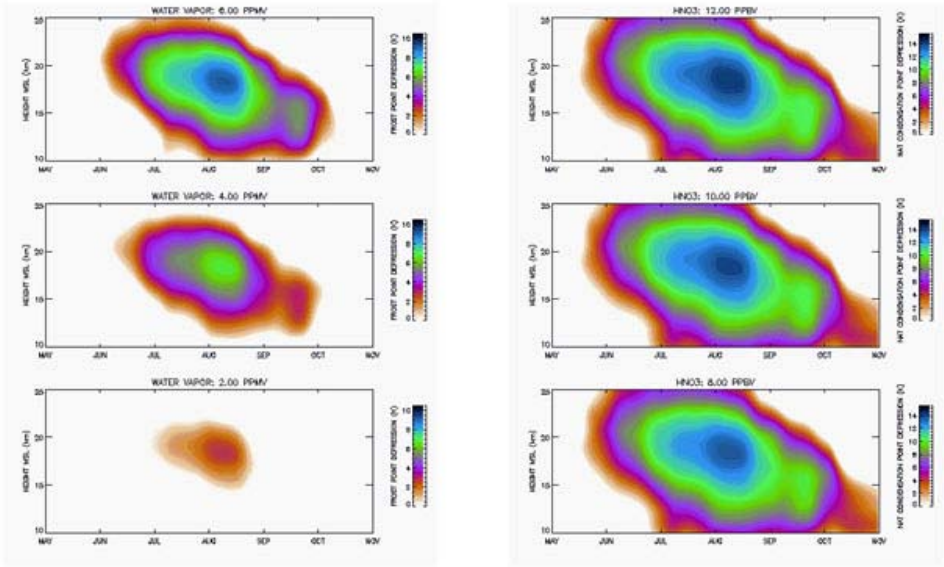

Figure 2. May to October 2003 at South Pole between 10 and 25 km MSL, frost-point depressions (K; left) for theoretical water-vapor mixing ratios of 6.0 (top), 4.0 (middle) and 2.0 ppmv (bottom) respectively, and nitric-acid trihydrate condensation point depressions (K; right) for mixing ratios of 12.0 (top), 10.0 (mid) and 8.0 (bottom) ppbv and a water-vapor mixing ratio of 4.0 ppmv.

vortex. Horizontal temperature gradients are at a maximum near 20 km over South Pole in August. Mixing would be least likely near these heights at this time. Ozone partial pressures measured by balloonsonde between 10 and 25 km MSL show that ozone loss rapidly occurred between 15 and 20 km beginning from early September. The spatial extent of the 2003 ozone hole was the second largest since measurements began. 2003 MPL PSC data are unique compared to measurements from 2004 and 2005 for the lack of PSC near 20 km MSL after mid-July. The ozone holes of 2004 and 2005 were relatively small compared to long-term averages.

Two alternate explanations for the lack of elevated clouds in the MPL data from July forward must be considered. First, we have used only a simple model for PSC formation. We do not take into account the potentially hydrophobic nature of embryonic haze particles coated with sulfuric and nitric acids. Second, cloud algorithm response may have been limited by the minimum ABR threshold. However, unattenuated backscatter ratio values for ice typically exceed 1.2 [*Gobbi et al.*, 1998]. It is likely that any occurrences of Type II PSC would have been detected. Some weakly scattering layers typical of Type I clouds, which have been observed to near 20 km into early September in past South Pole winters may have been missed.

4. REFERENCES

Campbell, J. R. D. L. Hlavka, E. J. Welton, C. J. Flynn, D. D. Turner, J. D. Spinhrine, V. S. Scott, and I. H. Hwang, Full-time, eye-safe cloud and aerosol lidar observation at Atmospheric Radiation Measurement program sites: Instruments and data processing, *J. Atmos. Oceanic. Technol.*, *19*, 431-442, 2002.

Campbell, J. R., E. J. Welton, J. D. Spinhirne, Q. Ji, S.-C. Tsay, S. J. Piketh, M. Barenbrug, and B. N. Holben, Micropulse lidar observations of tropospheric aerosols over northeastern South Africa during the ARREX and SAFARI 2000 dry season experiments, *J. Geophys. Rev.*, *108*(D13), 8497, doi:10.1029/2002JD002563, 2003.

Gobbi, G. P., G. Di Donfrancesco, and A. Adriani, Physical properties of stratospheric clouds during the Antarctic winter of 1995, *J. of Geophys. Res.*, *103*(D9), 10,859-10,873, 1998.

Pfenninger, M., A. Z. Liu, G. C. Papen, and C. S. Gardner, Gravity wave characteristics in the lower atmosphere at south pole, *J. Geophys. Res.*, *104*(D6), 5963-5984, 1999.

Toon, O. B., R. P. Turco, J. Jordan, J. Goodman, and G. Ferry, Physical processes in polar stratospheric ice clouds, *J. Geophys. Res.*, *94*, 11,359, 1989.

Welton, E. J., and J. R. Campbell, Micro-pulse lidar signals: Uncertainty analysis, *J. Atmos. Oceanic. Technol.*, *19*, 2089-2094, 2002.